Tectonically induced clastic-carbonate depositional sequences of the Pennsylvanian-Permian transition in the Rowe-Mora Basin, northern New Mexico

K. Krainer, S. G. Lucas, and B. S. Kues
2004, pp. 314-325. https://doi.org/10.56577/FFC-55.314

in:

Geology of the Taos Region, Brister, Brian; Bauer, Paul W.; Read, Adam S.; Lueth, Virgil W.; [eds.], New Mexico Geological Society 55 th Annual Fall Field Conference Guidebook, 440 p. https://doi.org/10.56577/FFC-55

This page is intentionally left blank to maintain order of facing pages.

TECTONICALLY INDUCED CLASTIC-CARBONATE DEPOSITIONAL SEQUENCES OF THE PENNSYLVANIAN-PERMIAN TRANSITION IN THE ROWE-MORA BASIN, NORTHERN NEW MEXICO

KARL KRAINER[1], SPENCER G. LUCAS[2] AND BARRY S. KUES[3]
[1]Institute of Geology and Paleontology, University of Innsbruck, Innrain 52, Innsbruck A-6020 AUSTRIA
[2]New Mexico Museum of Natural History, 1801 Mountain Road NW, Albuquerque, NM 87104
[3]Department of Earth & Planetary Sciences, University of New Mexico, Albuquerque NM 87131

ABSTRACT.— One of the few places in the late Paleozoic Rowe-Mora basin of northern New Mexico that preserves a section through the traditional Pennsylvanian-Permian boundary is near Canovas Canyon in the Sangre de Cristo Mountains, northwest of Las Vegas. At this section, the Alamitos Formation is ~ 172 m thick and has late Desmoinesian fusulinids in its lower part, and late Virgilian-Wolfcampian fusulinid and invertebrate macrofossils in its upper part. Macrofossil assemblages consist largely of crinoid and bryozoan fragments, and brachiopods (chiefly *Composita subtilita* and *Neosprifer dunbari*), indicating shallow, normal marine carbonate shelf depositional environments. The Alamitos Formation at Canovas Canyon was deposited on the northern part of the Pecos shelf and is composed of nonmarine (arkosic sandstone, conglomerate, and reddish-purple shale) and marine (shale and limestone) lithofacies. These lithofacies form six, well-developed asymmetrical transgressive-regressive (T-R) depositional sequences. There is much evidence of synsedimentary tectonics of the ancestral Rocky Mountain deformation in the Rowe-Mora basin during the Late Pennsylvanian, and formation of the Alamitos Formation depositional sequences at Canovas Canyon is interpreted as having largely been induced by tectonic movements. Eustatic sea-level changes caused by the Gondwana glaciation, which are responsible for cyclic sedimentation on tectonically stable shelf areas during the late Paleozoic, are interpreted as being of lesser importance in the Canovas Canyon section.

INTRODUCTION

In the ancestral Rocky Mountain foreland of northern New Mexico, the Rowe-Mora basin (also called Taos trough by many authors) developed during the Pennsylvanian as a complex intracratonic basin almost encircled by highlands of the ancestral Rocky Mountains (Fig. 1). As much as 3000 m of Pennsylvanian sediments are preserved in the Rowe-Mora basin, and these rocks are mostly of Morrowan-Desmoinesian age (Fig. 2). Upper Pennsylvanian strata, however, are rarely preserved in the southeastern Rowe-Mora basin because Lower Permian red beds generally rest with profound unconformity on Middle Pennsylvanian strata (Baltz and Myers, 1999). Indeed, there are few places in the basin where marine Upper Pennsylvanian-Lower Permian strata are preserved so that it is possible to study deposition in the Rowe-Mora basin across the system boundary.

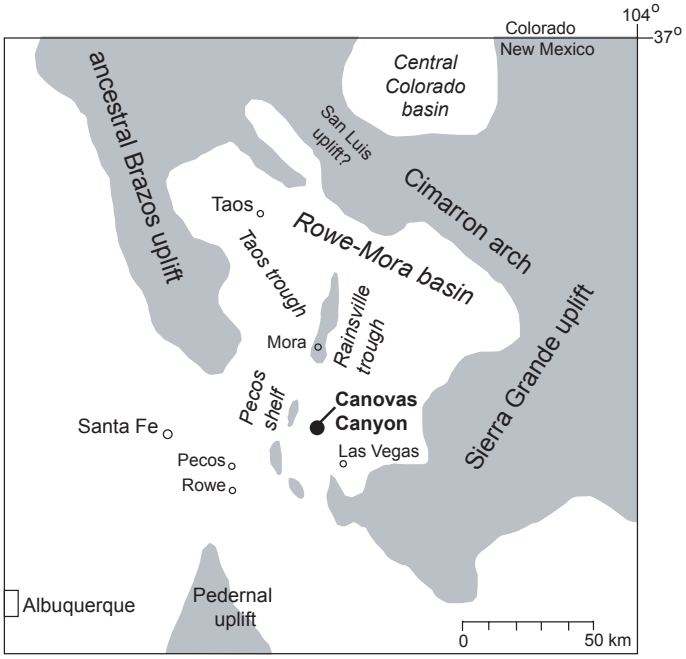

FIGURE 1. Simplified paleogeographic map of the Pennsylvanian Rowe-Mora basin in northern New Mexico (after Baltz and Myers, 1999) showing location of the Canovas Canyon section described here.

One such rare place is the outcrop belt just southeast of Canovas Canyon in the Sangre de Cristo Mountains northwest of Las Vegas (Fig. 1). This section is in the Rainsville trough of the Rowe-Mora basin. Here, forest roads expose strata of the Alamitos Formation that range from Desmoinesian through Wolfcampian in age. In this article, we present a detailed study of the lithostratigraphy, lithofacies, paleontology and sedimentation of the Alamitos Formation in the Canovas Canyon area. This study demonstrates that at this location, and presumably throughout the Rowe-Mora basin, sedimentation across the Pennsylvanian-Permian boundary was heavily influenced by local tectonism that overprinted the forcing mechanism of global eustasy.

LOCATION AND LITHOSTRATIGRAPHY

The section we studied (Fig. 3) was originally described by Baltz and Myers (1999, figs. 62, 81) as their section P. It is exposed along a forest road south of Gallinas Creek and New Mexico Highway 65 in the SE1/4 sec. 24, T17N, R14E. Baltz and Myers (1999) listed fusulinids and some macrofossil taxa from this section, and illustrated it (their figure 62) at a scale of 1 cm of diagram to about 20 m of section. We present here a much more detailed description of this section (Fig. 3) and complete documentation of its macroinvertebrate fossils.

This section encompasses the top of the Porvenir Formation, entire Alamitos Formation and base of the Sangre de Cristo

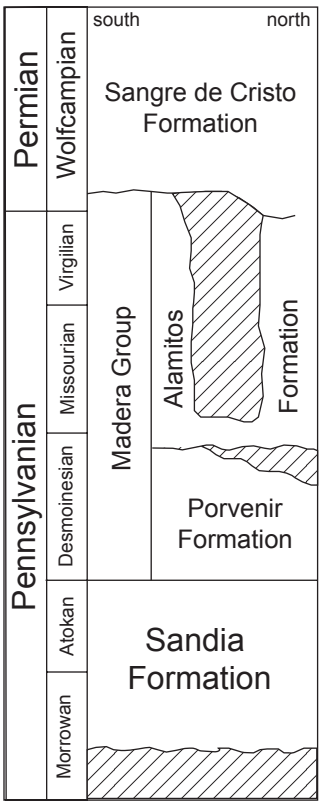

FIGURE 2. Summary of Pennsylvanian-Early Permian stratigraphy in the southeastern part of the Rowe-Mora basin (after Baltz and Myers, 1999).

Formation. The Alamitos Formation, as defined by Sutherland (1963), is interbedded arkosic sandstone, shale and marine limestone of Middle-Late Pennsylvanian (late middle Desmoinesian-Virgilian) age. According to Baltz and Myers (1999), the Alamitos Formation is about 200 m thick in the Canovas Canyon area and consists of more than 50% shale. Most of the formation is marine, but its sandstones, conglomerates and unfossiliferous red and purple shales may be of fluvial origin. Fusulinids indicate a late Desmoinesian to early Wolfcampian age.

At the section we measured (Fig. 3), the Alamitos Formation is a cyclic, mixed siliciclastic-carbonate succession approximately 172 m thick. This succession is composed of conglomerate and sandstone (comprising 17% of the section), siltstone and shale (43%) and limestone (10%). Covered intervals comprise 30% of the section.

LITHOFACIES OF THE ALAMITOS FORMATION

Conglomerate and Sandstone Facies

The base of the section (Fig. 3) is a 2.4-m-thick horizon of arkosic conglomerate and sandstone of the Porvenir Formation. The conglomerate contains quartz pebbles up to 3 cm in diameter, is poorly sorted and consists of angular to subrounded grains. The composition is mixed carbonate-siliciclastic (Fig. 4A). Carbonate grains are mostly micritic gray limestones frequently displaying pedogenic features (i.e., were formed in a terrestrial setting, and we refer to them as calcretes). Some micritic grains contain small recrystallized bioclasts (Fig. 4A). A thin, fine-grained, moderately to poorly sorted sandstone composed mostly of angular-subangular monocrystalline quartz, subordinate polycrystalline quartz and detrital feldspars is intercalated. Granitic and sedimentary rock fragments are rare, and a few micas are present. The sandstone is cemented by coarse, blocky calcite (Fig. 4B).

The base of the Alamitos Formation is a 2.3-m-thick coarse sandstone, rich in fine-grained matrix. The matrix-supported sandstone and underlying conglomerate at the top of the Porvenir Formation form the base of the lowermost cycle. Siliciclastic grains in the sandstone are mono- and polycrystalline quartz, granitic rock fragments, detrital feldspars and a few micas. Matrix is fine-grained micrite.

Within the Alamitos Formation, sandstones and fine-grained conglomerates commonly occur at the bases of the depositional sequences, abbreviated as DS below (Fig. 3). Their thickness varies, and increases from 1.1 m at the base of DS 2 to 6.4 m at the base of DS 6. In these coarse-clastic units at the bases of the DSs, a fining upward trend from fine-grained, sandy conglomerates to coarse, pebbly sandstone and medium-grained sandstone is observed. The bases of the conglomerate units are erosive; the maximum clast size is 5 cm, and trough crossbedding is common in both conglomerates and sandstones. Thinner sandstone layers (thickness 0.2-1.1 m) also occur within the DSs, intercalated with mudstone/siltstone. These sandstone intercalations are fine to coarse grained, and trough crossbedded, horizontally laminated or massive.

Throughout the section, sandstones are moderately to poorly sorted, containing angular to subangular grains (Fig. 4C). The most abundant grain type is monocrystalline quartz. Polycrystalline quartz is subordinate and composed of either a few large subindividuals (granitic) or many small subindividuals, which are rarely stretched (metamorphic). Detrital feldspars are abundant (> 15%), with potassium feldspar more abundant than plagioclase. Many feldspars are untwinned, perthitic feldspars, microclines or feldspars with polysynthetic and Karlsbad twins. Most feldspar grains are altered to different degrees, some being almost completely replaced by calcite or altered to phyllosilicates. Rock fragments are present in low percentages and consist of large subindividuals of quartz and feldspar (granitic), and of small subindividuals of muscovite and quartz (metamorphic). A few sandstones contain sedimentary rock fragments such as micritic limestone, reworked calcrete grains, and siltstone. These carbonate clasts are better rounded (subrounded to rounded) than the siliciclastic grains. Detrital micas are dominantly muscovite, subordinately biotite and are present in small amounts in all samples. Most sandstones contain fine-grained siliciclastic matrix rarely exceeding 10%. In some sandstones, detrital quartz grains display authigenic overgrowths, which are barely recognizable because of the lack of dark rims around the detrital grains. In a few sandstones, pore space is filled with microcrystalline quartz cement (chalcedony). Sandstones in the lower part of the section

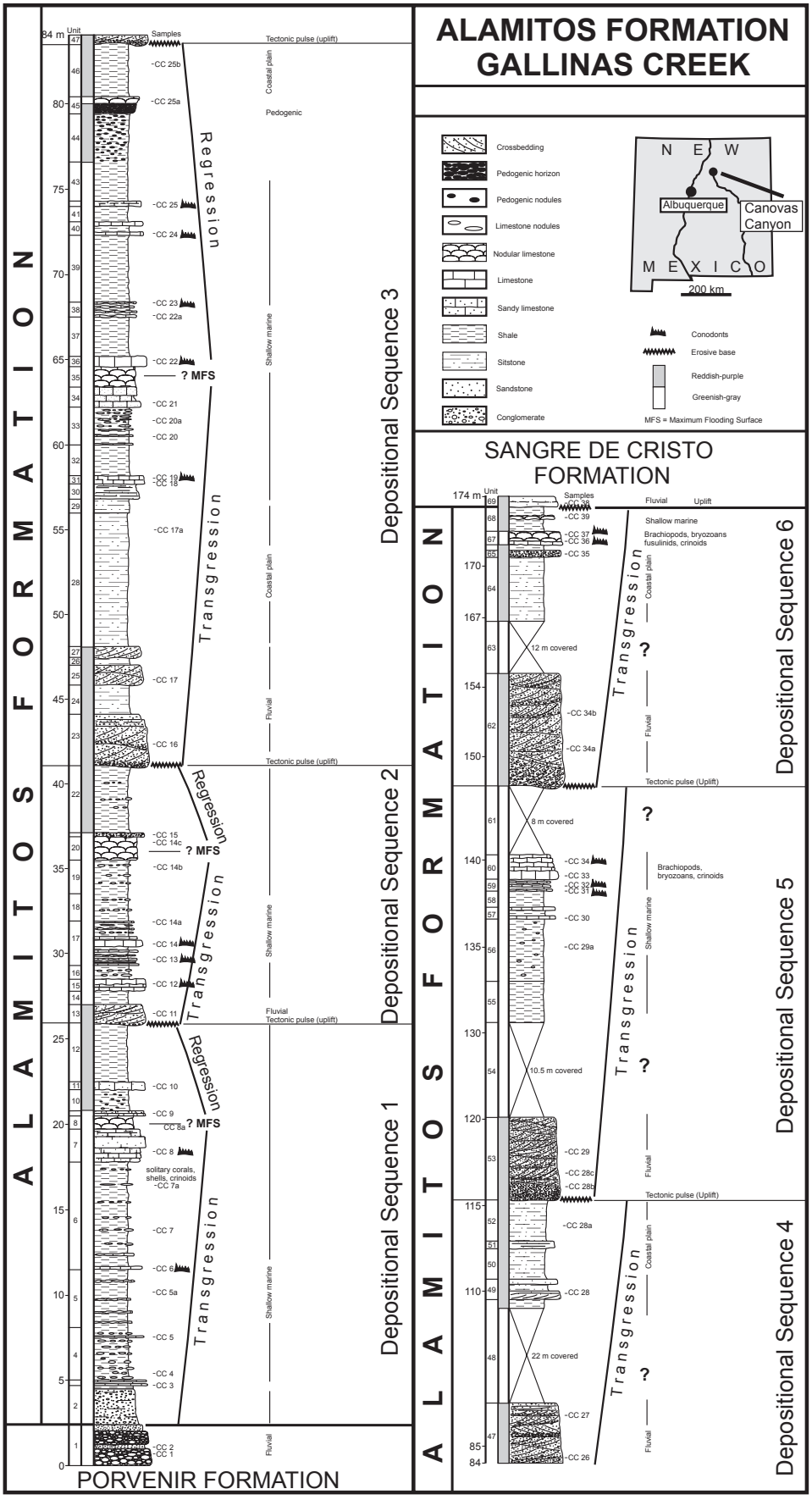

FIGURE 3. Measured section of the Alamitos Formation near Canovas Canyon.

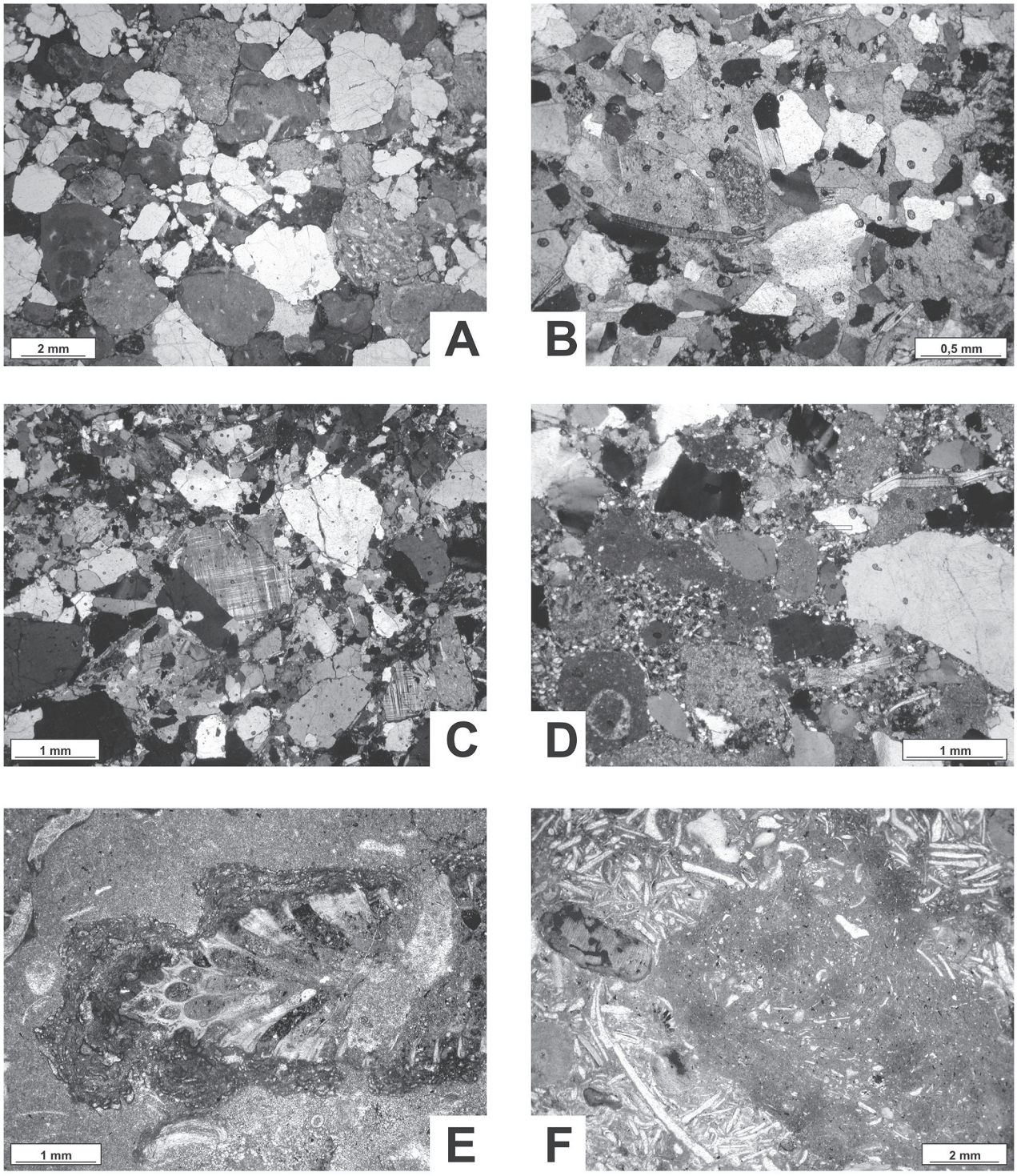

FIGURE 4. Thin section photographs of sandstones and limestones of the uppermost Porvenir Formation (A, B) and Alamitos Formation (C-F) near Canovas Canyon, southeastern Sangre de Cristo Mountains. A. Fine-grained, mixed siliciclastic-carbonate conglomerate containing abundant gray, micritic carbonate grains, detrital quartz and feldspar grains. Crossed nicols, Sample CC 1, Unit 1. B. Fine-grained sandstone composed of abundant detrital quartz grains, many feldspars and some detrital micas, cemented by coarse, blocky calcite cement. Crossed nicols, Sample CC 2, Unit 1. C. Coarse-grained, poorly sorted arkosic sandstone composed of detrital quartz and feldspar grains (mostly potassium feldspar). Crossed nicols, Sample CC 11, Unit 13 (base of DS 2). D. Coarse-grained arkosic sandstone composed of detrital quartz, some feldspars and abundant carbonate clasts, which rarely contain fossil fragments (lower left). The sandstone is cemented by coarse blocky calcite. Crossed nicols, Sample CC 35, Unit 65 (upper part of DS 6). E. Bioclastic wackestone containing a large bryozoan fragments which is encrusted by cyanobacteria (*Girvanella*) to form an oncoid grain. Plane light, Sample CC 31, Unit 59 (upper part of DS 5). F. Bioclastic wackestone with abundant recrystallized mollusc fragments, subordinate echinoderms and bryozoans, and micritic matrix. The rock is bioturbated. Plane light, Sample CC 34, Unit 60 (upper part of DS 5).

and at the base of the Sangre de Cristo Formation are cemented by coarse, blocky, pokilotopic calcite cement that randomly replaces detrital quartz and feldspar grains.

The coarse-grained pebbly sandstone layer at the base of the marine facies of DS 6 is arkosic, contains a few marine shell fragments, including crinoids and brachiopod spines, and is cemented by calcite (Fig. 4D). Due to their mineralogical composition and matrix content, the sandstones are defined as arkosic arenites (subarkoses and arkoses) according to the classification of Pettijohn et al. (1987).

Siltstone and Shale

In our measured section (Fig. 3), siltstone and shale are the most abundant lithotypes. In the lower part of the section (DS 1 to 3), greenish-gray, micaceous calcareous shale is the dominant lithotype, composed of different clay minerals (including kaolinite and illite), quartz, feldspar and calcite according to X-ray diffraction analysis. Within DS 1, about 15 m above the base, these shale intervals contain small solitary corals, shell debris and crinoid stem fragments, with many interbedded, thin, fossiliferous limestone beds, limestone lenses and nodules.

Reddish shales and siltstones are rare in the lower part of the section, but they occur in the uppermost part of DS 1 to 3. In DS 4 to 6, siltstones and shales are dominantly of reddish color, and subordinate greenish colors are present. Reddish siltstones and shales locally contain pedogenic carbonate nodules. The mineralogical composition is clay minerals, micas, quartz, potassium feldspar and plagioclase; calcite is absent.

Limestone

Limestones occur as thin limestone beds, mostly 5-20 cm thick, and as thin lenses and nodules intercalated in brownish-gray mudstone, particularly in DS 1 to 3. Individual limestone beds are up to 0.6 m thick, fossiliferous and gray, with wavy bedding.

The thickest limestone horizon is 1.4 m thick and consists of several wavy-bedded, gray limestone beds (DS 5). This limestone contains abundant brachiopods, crinoid stem fragments and bryozoans. The uppermost limestone beds in the upper part of DS 6 are nodular, gray, and fossiliferous, containing brachiopods (see below), crinoids, bryozoans and rare fusulinids. Many limestones (15 of 20 tested samples) yielded conodonts. Most samples contain only a few specimens, but a rich conodont fauna was obtained from samples CC13 and CC19.

According to J. Barrick (written commun., 2003), who examined our conodont samples, the most common conodont is *Adetognathus*, an undiagnostic shallow water form, but samples CC13 and CC14 also contain a couple of very small *Streptognathodus* and *Hindeodus*. Sample CC 34 yielded the most extensive conodont assemblage, with *Streptognathodus*, *Hindeodus* and *Ellisonia*. Within reddish siltstone and shale in the upper part of DS 1, 2 and 3, pedogenic limestone nodules are present; in DS 3 a nodular pedogenic limestone horizon is developed.

Bioclastic Wackestone/packstone

The most common microfacies of the limestones is bioclastic wackestone/packstone, locally grading into grainstone, and rarely rudstone. This facies is fine- to coarse-grained (rudstone), poorly sorted, nonlaminated, and locally bioturbated (Fig. 4F). Among the skeletal grains, recrystallized shell fragments derived from brachiopods, bivalves, small gastropods, echinoderm fragments (mostly crinoids) and bryozoans are most abundant (Figs. 5D, F). Brachiopod and echinoid spines, ostracods, and trilobite fragments are subordinate. Smaller foraminifers (*Globivalvulina, Endothyra, Hemigordius, Syzrania, Tetrataxis, Tuberitina*, calcivertellids) are rare to very rare. In samples 19 and 30, a few fragments of dasycladacean algae (?*Epimastopora*) are present. In some wackestones, skeletal fragments are encrusted by cyanobacteria, rarely by sessile foraminifers. Rarely bryozoans are encrusting echinoderm fragments.

In limestones of DS 5 and 6 (samples 30, 31, 39), many bioclasts (shell fragments, echinoderms, brachiopod spines, bryozoans) are encrusted by cyanobacteria forming small oncoids (Fig. 4E). Non-skeletal grains are small, angular quartz grains, a few micas and detrital feldspars, a few micritic carbonate grains rarely containing small bioclasts, a few phosphoritic grains, and peloids. The matrix is recrystallized brownish micrite, and some calcite cement is present in small voids.

Spicular Wackestone

An unusual wackestone type is fine grained and contains abundant sponge spicules, many smaller foraminifers (mostly calcivertellids, rare *Tuberitina, Endothyra* and others), ostracods, and peloids (Fig. 5E). A few larger skeletons, such as echinoderms, bivalves, brachiopods, gastropods and bryozoans, are present. Skeletons and peloids are embedded in micritic matrix, and the rock is bioturbated.

Skeletal Grainstone/packstone

Skeletal grainstone/packstone is rare. This microfacies is coarse grained, poorly sorted, nonlaminated and calcite cemented. Larger bioclasts are mostly echinoderms (crinoids); less abundant are recrystallized shell fragments and bryozoans (Figs. 5A, C). A few trilobite fragments and ostracods are present. Smaller skeletal grains are mostly coated grains (recrystallized small bioclasts coated by dark micritic envelopes) and micritic grains (intraclasts). Siliciclastic grains are abundant, particularly mono- and polycrystalline quartz, and, subordinately, altered detrital feldspars are present (Fig. 5A).

Oolitic Grainstone

Oolitic grainstone is very rare (Fig. 5B), occuring only in unit 15. This facies is well to moderately sorted and nonlaminated. Ooids are radial concentric with radial calcite fabric, mostly 0.2 to 0.5 mm in diameter. The nucleus of the ooids is formed by

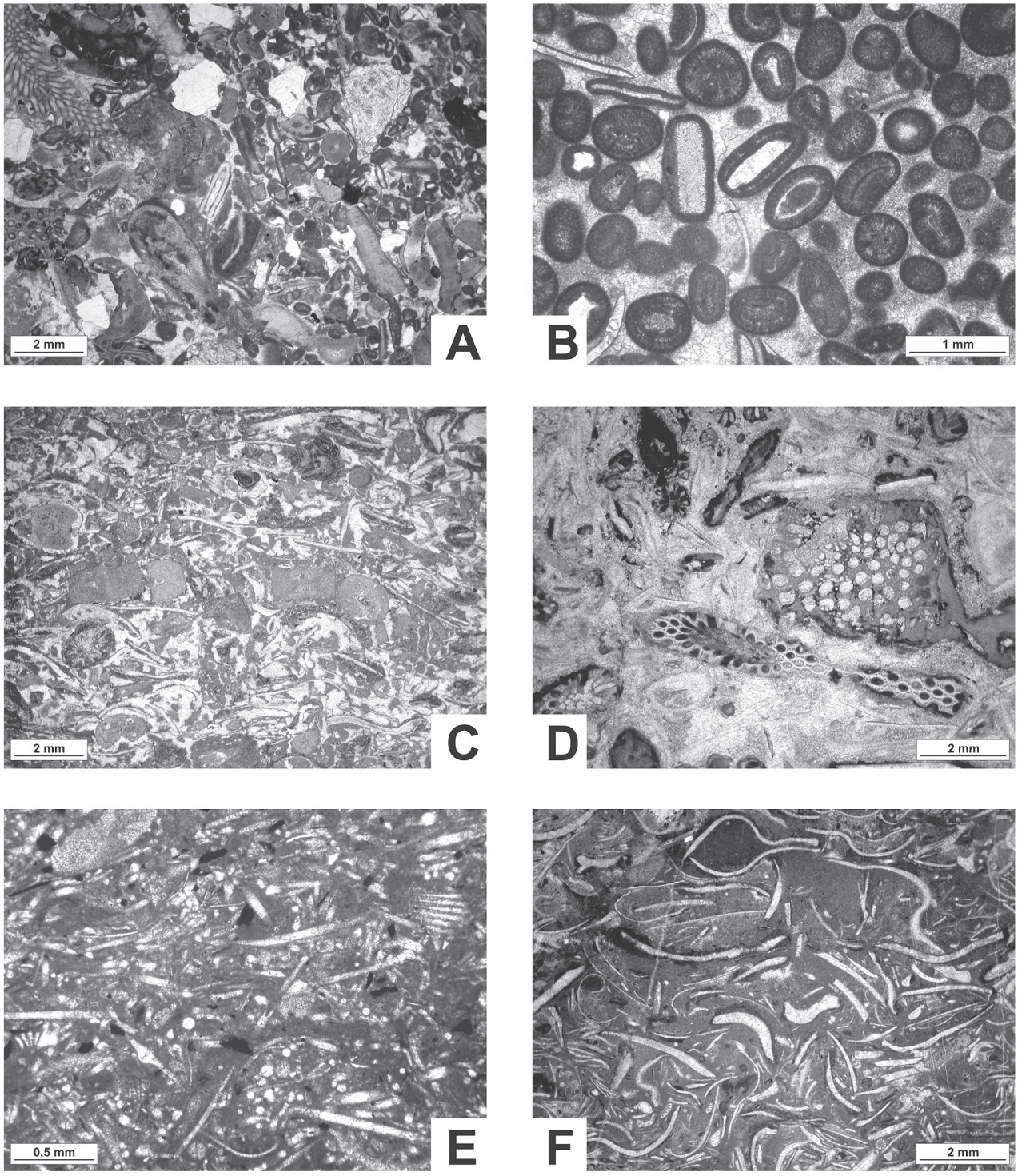

FIGURE 5. Thin section photographs of limestone microfacies of the Alamitos Formation near Canovas Canyon, southeastern Sangre de Cristo Mountains (all plane light). A. Coarse-grained and poorly sorted packstone containing abundant crinoid fragments, mollusc debris and bryozoans. Many skeletons display dark gray, thin micritic envelopes. A few detrital quartz grains are present. Sample CC 10, Unit 11 (upper part of DS 1). B. Oolithic grainstone, well sorted, with well developed radial-concentric ooids and a few skeletons, cemented by calcite. Sample CC 12, Unit 15 (lower part of DS 2). C. Bioclastic grainstone composed of recrystallized shell debris, echinoderms, a few bryozoans and ostracods, cemented by calcite. Some micritic matrix is present. Sample CC 14, Unit 17 (DS 2). D. Bioclastic wackestone/rudstone, poorly sorted, containing abundant bryozoan fragments, most of them showing thin micritic envelopes. Subordinate shell debris and echinoderm fragments are present. Matrix is recrystallized micrite, some calcite cement is also present. Sample CC 25, Unit 42 (upper part of DS 3). E. Bioclastic wackestone with abundant spicules ("spiculite") embedded in gray micritic matrix. Subordinate ostracods, shell debris and echinoderm fragments are present. Sample CC 20a, Unit 33 (middle part of DS 3). F. Bioclastic wackestone composed of abundant recrystallized shell fragments derived from bivalves, brachiopods and rarely small gastropods. Some other skeletons are present. Matrix is gray micrite. Many skeletons display thin, dark gray micritic envelopes. Sample CC 23, Unit 38 (middle part of DS 3).

bioclasts (shell fragments, rare smaller foraminifers, small gastropods), quartz grains and small micritic grains. Skeletal grains are present in small amounts, including large shell fragments with thin micritic envelopes, echinoderms, ostracods, gastropods and rare bryozoans. Non-skeletal grains such as angular quartz grains and detrital feldspars are rare.

Facies Interpretation

Textural and structural properties of the sandstones and conglomerates at the base of each DS, including erosional bases, trough crossbedding, poor sorting and rounding, and siliciclastic matrix, indicate a fluvial origin (multistoried channel fills). The siliciclastic material is derived mostly from granitic, and subordinately from metamorphic source rocks. Poor sorting and angularity of the larger clasts indicate short transport distances. The thin, coarse-grained, arkosic sandstone layer below the limestones in the upper part of DS 6, which contains abundant reworked limestone clasts, a few skeletal grains and calcite cement, probably formed in a shallow marine, high energy environment during rapid transgression.

We interpret the reddish shales and siltstones as terrigenous deposits, probably of a flat coastal plain or distal alluvial plain. Carbonate nodules and nodular limestone horizons within the reddish siltstone and shales are interpreted as pedogenic calcrete nodules and calcrete crusts. The greenish-gray mudstones and siltstones with thin, intercalated limestone beds, lenses and nodules that locally contain marine fossils are deposits of a shallow marine environment.

Limestones that contain a diverse marine fauna, including conodonts, point to a shallow open marine depositional environment with normal salinity. Skeletal wackestones and packstones containing abundant lime mud, a diverse fauna and bioturbation, were deposited in an open marine environment below fair weather wave base. Thin packstone/grainstone layers most probably represent storm layers. Skeletal grainstones formed in a higher energy environment such as wave-agitated skeletal banks. We assume the oolitic grainstone formed on high-energy, shallow water sandshoals. The spicular wackestone, characterized by a low diversity benthic fauna, is interpreted by us to have been deposited in a low-energy environment below the fair weather wave base, probably also below the storm wave base.

PALEONTOLOGY

Baltz and Myers (1999) reported two macroinvertebrate localities in argillaceous limestones near the top of the Alamitos Formation in their section P, near Canovas Canyon. Both localities were sampled during this study, together with additional collections made from equivalent units a short distance to the south, at the top of section 6 of Baltz and Myers (1999, fig. 81). Their two section P collections were 27403-PC, just below the uppermost Alamitos bed, containing the fusulinid *Triticites* aff. *T. creekensis* Thompson, and 27503-PC, about 20 m below the unit containing 27504-PC. The unit containing collection 27504-PC is equivalent to beds 66 and 67 (NMMNH locality 5583) of our section (Fig. 3), and 27503-PC is from bed 60 (NMMNH locality 5581) of our section. Preservation of the fossils from all localities is rather poor, with weathering and calcitic encrustation often obscuring the surface features of the specimens. Here, we briefly describe the macroinvertebrates from these localities and illustrate some of the most characteristic taxa (Fig. 6).

Bed 60, a medium gray limestone, contains dense accumulations of shell material, ranging from complete shells to fine shell fragments of marine invertebrates, some of which weather free on the outcrop. Locally within these limestones, bioclasts may comprise more than 50 percent of total rock volume. Crinoid stem fragments and a moderate variety of bryozoan and brachiopod taxa are the main constitutents of the bed 60 fauna. Bryozoans include relatively large, coarsely branched fragments (possibly of *Tabulipora*), and lower numbers of small rhomboporoid and fenestrate fragments.

Brachiopods are dominated numerically by specimens of *Composita subtilita* (Hall) and *Neospirifer dunbari* King, both of which are far more abundant than any other brachiopod taxa. Specimens of *Composita subtilita* (Figs. 6A-C) are mostly the typical morph, slightly longer than wide, and attain a maximum length of about 25 mm. Their size ranges down to juvenile specimens less than 10 mm long (e.g., Fig. 6C). *Neospirifer dunbari* (Fig. 6D) is characterized by moderate size for the genus (width up to about 50 mm), relatively few (up to 11) plicae in the sulcus, including an unbranched central M-plica, and plicae on the lateral portions of the valves that are relatively coarse and do not branch much, so that no more than three plicae are present in the fascicles nearest the fold and sulcus. One *Neospirifer* specimen (Fig. 6F) is unusually alate (length = 26 mm; width = 51 mm) and possesses plicae that are finer than is typical of *N. dunbari*. This specimen appears to be related to *N. alatus* Dunbar and Condra, a species observed in the Missourian but not Virgilian of the Sangre de Cristo Mountains by Sutherland and Harlow (1973). A second spiriferid is the small (maximum width = 12 mm), strongly and simply plicate genus *Punctospirifer* (Fig. 6G). These specimens are not as wide as is typical of the common New Mexico species *P. kentuckyensis* (Shumard), but may fall into the considerable range of variability that has been documented for that species.

Productoid brachiopods are uncommon, consisting only of poorly preserved specimens of *Linoproductus* sp. (Fig. 6H) and *Parajuresania* cf. *P. nebrascensis* (Owen) (Fig. 6I). The only other brachiopod recovered from bed 58 is a single incomplete specimen of *Phricodothyris* cf. *P. perplexa* (McChesney) (Fig. 6J). *Crurithyris* sp. and *Derbyia* sp. were reported by Baltz and Myers (1999, table 5) from this locality but were not observed by us.

Molluscs are rare in the bed 58 assemblage and are limited to bivalves. The only identifiable specimens are the small (length = 5 mm) nuculoid *Nuculavus* sp. (Fig. 6K) and several fragments of *Acanthopecten* (Fig. 6L). *Acanthopecten* is characterized by strong, simple radial ribs that are interrupted during growth by conspicuous concentric lamellae that are vaulted over the ribs. The upper Alamitos specimens are convex left valves, and their ribs are broad and somewhat sharp crested, with the lamellae arched across them. These features suggest assignment to *A.*

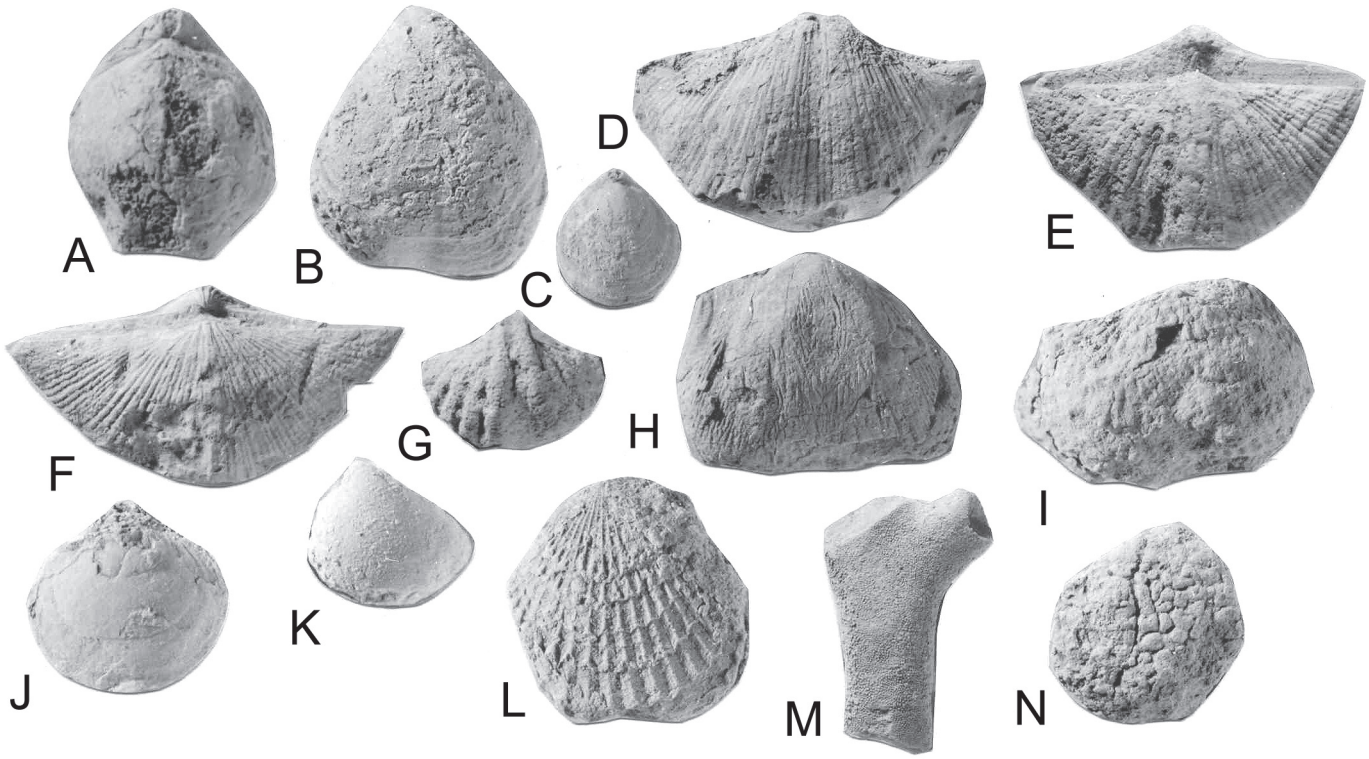

FIGURE 6. Invertebrates from the uppermost Alamitos Formation, Canovas Canyon area, New Mexico. Brachiopods, A-J; bivalves, K, L; bryozoan, M; algae, N. Specimens A-D, F-L from locality 5581; E, N, from locality 5584; M from locality 5582. A-C, *Composita subtilita* (Hall). A, brachial valve view, NMMNH P-42138, x1.5; B, pedicle valve, NMMNH P-42139, x1.5; C, brachial view of juvenile specimen, NMMNH P-42140, x2. D, E, *Neospirifer dunbari* King. D, pedicle valve, NMMNH P-42141, x1; E, brachial view, NMMNH P-42142, x1. F, *Neospirifer* aff. *N. alatus* Dunbar and Condra, brachial valve view, NMMNH P-42143, x1. G, *Punctospirifer* cf. *P. kentuckyensis* (Shumard), pedicle valve, NMMNH P-42144, x2.5. H, *Linoproductus* sp., highly weathered pedicle valve, NMMNH P-42145, x1.5. I, *Parajuresania* cf. *P. nebrascensis* (Owen), incomplete poorly preserved pedicle valve, NMMNH P-42146, x1.8. J, *Phricodothyris* cf. *P. perplexa* (McChesney), incomplete brachial valve, NMMNH P-42147, x2. K, *Nuculavus* sp., right valve, NMMNH P-42148, x 4.5. L, *Acanthopecten meeki* Newell, left valve, NMMNH P-42149, x 3. M, bryozoan, fragment of coarsely branched zoarium, NMMNH P-42150, x1. N, encrusting algae (*Ottonosia*?), NMMNH 42151, x1.

meeki Newell rather than to *A. carboniferus* (Stevens), which has a flatter left valve, and lower and more continuous ribs, each having a discrete fine costella along its crest. Both species are known from the Virgilian of the Midcontinent (Newell, 1937) and north-central New Mexico (Kues, 1996). Baltz and Myers (1999, table 5) also reported the bivalves *Astartella*? sp. and *Myalina (Orthomyalina)* sp. from this locality.

Near the top of the Canovas Canyon Alamitos section (section P, collection 27504-PC of Baltz and Myers, 1999), beds 66 and 67 of our section (locality NMMNH 5583; Fig. 3) are beds of medium gray limestone, which contains abundant bioclastic shell debris, although not to the extent of bed 60. The fauna is similar in containing abundant crinoid stem segments, the same kinds of bryozoans, and common *Neospirifer dunbari* and *Composita subtilita*, as well as *Punctospirifer* cf. *P. kentuckyensis* and *Parajuresania nebrascensis* among the brachiopods. A few echinoid spine fragments were also observed in this assemblage. Additional brachiopods not observed in bed 58 include *Antiquatonia*? sp. and *Echinaria* cf. *E. moorei* (Dunbar and Condra). The latter species is moderately common in beds 66-67, but is represented mainly by brachial valve fragments. These valves have an estimated maximum width of about 45 mm when complete. Pedicle valves display the characteristic narrow concentric bands and, within each band, about three irregular transverse rows of small prostrate spines. These specimens may be the taxon reported by Baltz and Myers (1999) as *Calliprotonia*? sp., a genus that is externally similar to *Echinaria*. However, *Calliprotonia* has lateral ridges along the hingeline of the interior of the brachial valve that extend around the lateral and anterior margins of the valve (e.g., Muir-Wood and Cooper, 1960), whereas the lateral ridges of *Echinaria* are restricted to the hingeline, as in the Alamitos specimens. In addition, the Alamitos specimens display the bilobate cardinal process characteristic of *Echinaria*, whereas *Calliprotonia* possesses a trilobate process. Baltz and Myers (1999, table 5) also reported *Cleiothyridina*? sp. from collection 27504-PC, a brachiopod not present in our collections, and reported no bivalves. The only bivalve remains we observed were partial external molds of the large, elongate valves of *Wilkingia terminale* (Hall).

Collections from section 6 of Baltz and Myers (1999, fig. 81), about 0.7 km to the south along Johnson Mesa road, were made from two limestone units near the top of the Alamitos Formation.

The lower of these units (NMMNH locality 5584) yielded the same fauna as bed 60 of our Gallinas Creek section, and is the same unit. As in bed 60, *Composita* and *Neospirifer* (Fig. 6E) are the most abundant brachiopods, and shells encrusted with knobby algae (*Ottonosia*?; Fig. 6N) are common. Higher in this section, a few meters below the basal sandstone of the Sangre de Cristo Formation, NMMNH locality 5582 yielded a similar fauna, with fewer brachiopods (again, mostly *Composita* and *Neospirifer*) and a greater abundance of bryozoans, especially fragments of large coarsely-branched forms (Fig. 6M). Baltz and Myers (1999) collected no macroinvertebrates from these localities, reporting only the fusulinids *Triticites* aff. *T. ventricosus*, *T.* aff. *T. creekensis*, and *Oketaella*? sp. from the upper 20 m of the Alamitos in their section 6.

All of the faunas reported here consist predominantly of brachiopods, and crinoid and bryozoan fragments, which are stenohaline groups that lived in conditions of stable normal marine salinity. *Composita* occurs widely in limestone and shale facies representing a variety of shallow marine environments in the Late Pennsylvanian of New Mexico. Studies of late Paleozoic faunas elsewhere (e.g., Stevens, 1971; Rollins et al., 1979) suggest that *Neospirifer* characterizes maximum transgressive phases and stable offshore marine carbonate environments that also supported abundant crinoid and bryozoan faunas. However, the highly fragmented, randomly oriented, bioclastic concentrations in the upper Alamitos limestones reported here indicate that these assemblages were transported and concentrated in shallow water above wave base, probably close to the shoreline. They represent the last marine environments in this area of the Rainsville trough prior to the complete inundation of the area by nonmarine siliciclastic red beds of the Sangre de Cristo Formation.

AGE

The lower part of the Alamitos Formation in the Canovas Canyon area yields late Desmoinesian fusulinids (Baltz and Myers, 1999). Baltz and Myers (1999, p. 116-119) discussed the age of the upper Alamitos Formation in the southeastern Sangre de Cristo Mountains, including the Canovas Canyon area, and noted that the youngest fusulinids (e.g., *Triticites creekensis*) indicate an early Wolfcampian age. The fusulinids correlate with those found in the upper part of the La Casa Member, Wild Cow Formation, and lower part of the overlying Bursum Formation (Madera Group) in the Manzano Mountains (e.g., Myers, 1988). *Triticites creekensis* also occurs in the lower half of the Bursum Formation at its type section, in the northern Oscura Mountains of Socorro County, but also ranges downward into underlying Virgilian strata (Lucas et al., 2000). Therefore, the fusulinids from near the top of the Alamitos Formation in the Canovas Canyon area indicate a latest Virgilian or an early Wolfcampian age.

Recent reevaluation of the position of the Virgilian (Pennsylvanian)-Wolfcampian (Permian) boundary in the Midcontinent and New Mexico/west Texas areas by some workers (e.g., Wahlman, 1998; Sanderson et al., 2001) suggests that species such as *T. creekensis* and others traditionally considered part of Bursum assemblages and of early Wolfcampian age should be considered Pennsylvanian (latest Virgilian) rather than Permian in age. However, a traditional interpretation of the biostratigraphy would regard them as early Wolfcampian and Early Permian in age, and we follow that interpretation here.

The identifiable macroinvertebrates of the upper Alamitos are also indicative of a late Virgilian or early Wolfcampian age, but do not allow any greater precision. Thus, the Alamitos section at Canovas Canyon spans the interval late Desmoinesian through possibly early Wolfcampian, and may cross the (traditional) Pennsylvanian-Permian boundary (Fig. 7). It is worth noting that two of the brachiopod genera present in the upper Alamitos Formation—*Punctospirifer* and *Phricodothyris*—are not known in New Mexico in Bursum-age (early Wolfcampian) strata, so this may be evidence of a late Virgilian age for the upper part of the Alamitos Formation in the Canovas Canyon area. However, the most that can be said with certainty is that the top of the Alamitos Formation in the Canovas Canyon area is close in age to the Virgilian-Wolfcampian boundary.

DEPOSITIONAL SEQUENCES

In the Alamitos Formation section at Canovas Canyon, the nonmarine and marine lithofacies described above form six, well-developed asymmetrical transgressive-regressive (T-R) depositional sequences (Fig. 7). Sequence thickness ranges from 15.1 m (DS 2) to 42.5 m (DS 3). The lower three sequences are composed of thick transgressive deposits, overlain by thin regressive deposits; in the upper three depositional sequences, the regressive deposits are lacking. The bases of all sequences are formed by fluvial sandstones and conglomerates, which erosively overlie fine-grained marine or nonmarine shales and siltstones. These major facies changes arguably represent sequence boundaries, caused by a rapid fall in relative sea-level and the development of a subaerial unconformity. The fluvial sandstones and conglomerates at the bases of the depositional sequences were probably deposited immediately after the sea-level fall, when sea-level began to rise (lowstand systems tract, LST).

Marine shales and intercalated limestones that overlie this fluvial facies were deposited during rising sea-level, representing the transgressive systems tract (TST). The top of the TST is commonly documented by the maximum flooding surface (MFS), which separates the TST from the overlying highstand systems tract (HST). In many sections the MFS is represented by a condensed section, which formed during the maximum landward extension of marine conditions.

In DS 1and 2 the MFS is probably represented by thin nodular limestone intervals that are assumed to document the most landward distribution of open marine limestones (Fig. 7). A nodular limestone that is under- and overlain by thin limestone beds composed of wackestone, locally spicular wackestone, and containing abundant conodonts, is regarded as the MFS of DS 3. In DS 1-3, limestones of the MFS are overlain by thin intervals of marine shale/siltstone and intercalated limestone beds (bioclastic wackestone/packstone/grainstone), grading into nonmarine red-

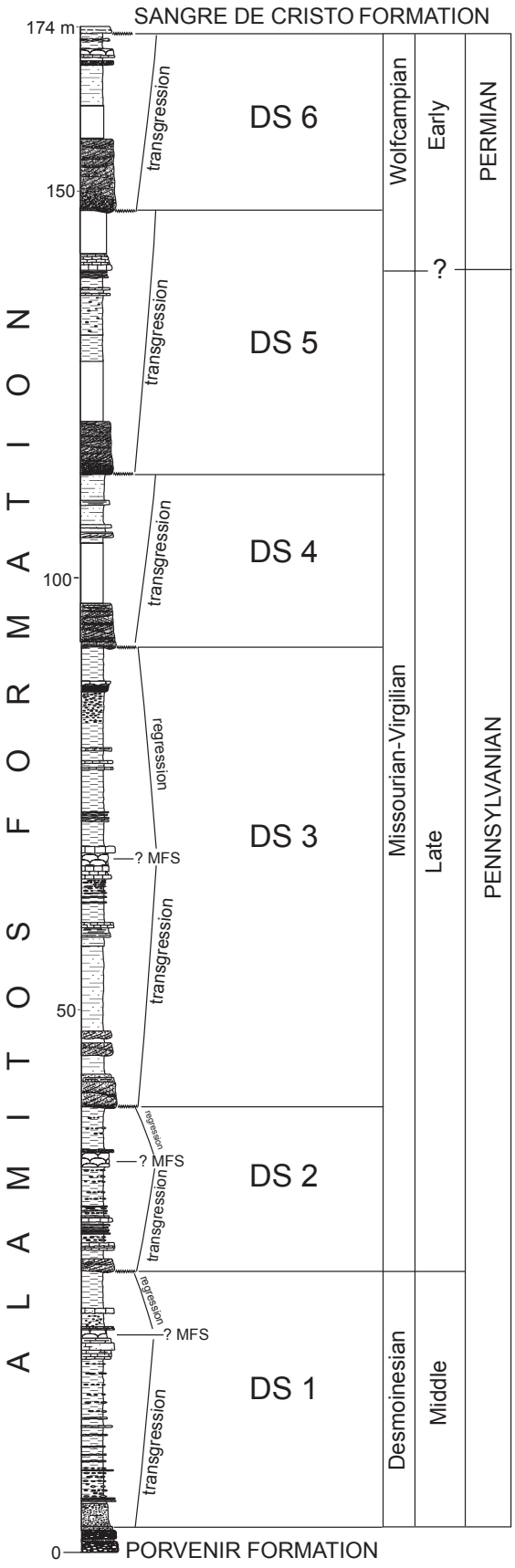

FIGURE 7. Summary of sequence stratigraphy and age of Canovas Canyon section.

dish shale/siltstone of a coastal or distal alluvial plain environment locally containing calcrete nodules and a pedogenic nodular limestone bed in DS 3.

These regressive successions developed on top of DS 1-3 are interpreted as deposits of the highstand systems tract, where the marine facies represents the early highstand and the overlying nonmarine fine-grained deposits resulted from progradation of the highstand deposits (late highstand). Above these highstand deposits, a significant fall in sea-level caused erosion and formation of a type 1 sequence boundary, overlain by coarse fluvial deposits of the next DS.

DS 4 is a nonmarine, fining-upward sequence consisting of the coarse fluvial facies at the base, grading into nonmarine shales and siltstones with thin, intercalated coarse-grained arkosic sandstone layers. This DS lacks marine deposits, and the fine-grained nonmarine facies is erosively overlain by coarse fluvial deposits of the next cycle.

The uppermost two sequences, DS 5 and 6, are likewise transgressive successions lacking the regressive deposits on top (Fig. 7). Both cycles consist of coarse-grained fluvial facies (LST), grading into red and greenish siltstone/shale of a distal alluvial plain or coastal plain setting and finally into green marine shale with intercalated fossiliferous limestone of a shallow, open marine environment (TST).

The marine facies consists of stacked facies associations of alternating marine shale and thin limestone beds with shale intercalations. Such facies associations composed of thin packages of strata are recognizable in DS 1, 2, 3, and 5, indicating a change in the local depositional environment.

Stacked facies associations within depositional sequences are frequently termed parasequences. According to the nomenclature of sequence stratigraphy, parasequences are generally upward-shoaling successions composed of vertical facies associations with either an upward-coarsening or upward-fining trend, which records a gradual decrease in water depth. Parasequences are bounded by marine flooding surfaces or correlative surfaces with evidence of an abrupt change in water depth, commonly associated with minor submarine erosion or nondeposition, and with a minor hiatus (e.g. , Emery and Myers, 1996; Van Wagoner et al., 1999). As neither a clear fining-upward or coarsening-upward trend nor such a marine flooding surface is recognizable within the stacked facies associations of the depositional sequences of the Alamitos Formation, it is not possible to further subdivide the depositional sequences into parasequences.

TECTONICS AND SEDIMENTATION

During the Pennsylvanian, sedimentation in the Rowe-Mora basin and on the Pecos shelf (Fig. 1) was strongly influenced by tectonic movements that resulted in strong vertical and lateral variations in facies and thickness (e.g., Sutherland, 1963, 1972; Casey 1980; Baltz and Myers, 1999). Sutherland (1963) and Baltz and Myers (1999) stated that the sandstones and conglomerates of the Alamitos Formation contain high amounts of fresh, unweathered feldspars. However, our thin section analysis shows that most detrital feldspar grains are altered to various

degrees, and some are almost completely altered to clay minerals or replaced by calcite. Nevertheless, this alteration occurred after deposition due to diagenetic processes. Originally, the feldspar grains were deposited as relatively unweathered, fresh detrital grains, indicating rapid transport and deposition from a nearby granitic source area.

At the type section near Pecos, the Alamitos Formation is 390 m thick; it is 197 m thick in the Gallinas Creek area (Baltz and Myers, 1999) and 172 m thick at the section described here. Locally, between the Rita Cebolla and Mora River, thickness decreases to only about 30 m, and the Alamitos Formation is locally absent south of Montezuma (Baltz and Myers, 1999). North and northwestward, in the Rowe-Mora basin close to the Picuris-Pecos fault, thickness increases considerably, and in the Rio Pueblo area the Alamitos is about 1219 m thick, although its age is restricted to late Desmoinesian (Sutherland, 1963).

The Alamitos Formation of the Canovas Canyon area was deposited on the northeastern margin of the Pecos shelf, which graded northward into the Taos trough, a small elongate, north-south-trending basin that formed in response to the ancestral Rocky Mountain deformation and was tectonically active during Late Pennsylvanian time (Casey 1980, Kluth and Coney, 1981; Soegaard, 1990; Baltz and Myers, 1999). Major tectonic movements occurred, particularly along the Picuris-Pecos fault, elevating the Uncompahgre uplift at the western side of the fault during the late Desmoinesian so that it remained high throughout the Pennsylvanian (Sutherland, 1963). According to Kottlowski (1968), the northern part of the Pedernal uplift, which bounded the Pecos Shelf to the south, was also a source area for clastic sediment supply to the Pecos shelf.

On the Pecos shelf, marine sediments, including shelf carbonates, prograded towards the north and west during periods of tectonic quiescence and reduced clastic input. Coarse clastic sediments formed in response to episodic movements, particularly along the Picuris-Pecos fault, causing increased erosion of the uplifted areas and transportation of huge amounts of coarse clastic sediments and rapid progradation of braided streams toward the south and southeast across the shallow shelf.

There is also evidence that the Cimarron arch was periodically uplifted during Middle and Late Pennsylvanian time (Baltz, 1965; Casey, 1980). According to Sutherland (1963), the Pecos shelf area was disrupted by local faulting or folding during Late Pennsylvanian/Early Permian time, causing local uplift and erosion of the Alamitos and La Pasada formations and deposition of the Sangre de Cristo Formation on older formations. Baltz and Myers (1999) report that the anticline between the Rito Cebolla and Mora River was tectonically active during Desmoinesian and Late Pennsylvanian time, influencing deposition of the Alamitos Formation to the north and south.

According to Baltz and Myers (1999), in the Canovas Canyon area the clastic material is derived from nearby granitic Precambrian basement rocks, most probably west or north of the present outcrops. The relatively thin succession of the Alamitos Formation of the Canovas Canyon area is of late Desmoinesian-early Wolfcampian age, and thus was deposited during a relatively long period that encompasses the entire Missourian and Virgilian, at least six million years (Heckel, 2003). In the Midcontinent, there are more than 70 glacioeustatic cycles positioned for the Missourian-Virgilian interval (Heckel, 2003), approximately ten times as many cycles as are preserved in the Canovas Canyon section. This indicates the presence of considerable gaps (periods of nondeposition, more likely of erosion) at the erosive bases (sequence boundaries) of each Alamitos depositional sequence, caused by episodic synsedimentary tectonic movements related to ancestral Rocky Mountain deformation.Varying thickness of the depositional sequences and the presence of considerable gaps of unknown duration and most likely of varying duration (as well as condensed intervals of section) argue for episodic rather than periodic, synsedimentary tectonic movements.

There is much evidence of synsedimentary tectonics of the ancestral Rocky Mountain deformation in the Rowe-Mora basin during the Late Pennsylvanian, and formation of the Alamitos Formation depositional sequences at Canovas Canyon was arguably induced by tectonic movements. Episodic tectonic uplift caused transportation of huge amounts of coarse clastic debris into the Rowe-Mora basin and onto the Pecos shelf and rapid progradation of fluvial braidplain deposits towards the south and east across the shelf. During periods of tectonic quiescence and reduced siliciclastic input, shallow marine conditions prevailed on the shelf and prograded towards the north and west. Eustatic sea-level changes caused by the Gondwana glaciation, which are responsible for cyclic sedimentation on tectonically stable shelf areas during the late Paleozoic, were thus of minor importance in the Canovas Canyon section. The stacked facies pattern of alternating marine shale and limestone with shale intercalations in some of the depositional sequences is probably the result of such eustatic sea-level changes. The lack of clear fining-upward or coarsening-upward trends within these facies successions may be explained by tectonic activity overprinting the eustatic sea-level changes.

ACKNOWLEDGMENTS

Jess Hunley and Sally Johnson provided valuable field assistance. Jim Barrick identified conodonts and Felix Heller prepared the thin sections. Bruce Allen, Bob Colpitts and Bill Raatz provided helpful comments on the manuscript.

REFERENCES

Baltz, E. H., 1965, Stratigraphy and history of Raton Basin and notes on San Luis Basin, Colorado-New Mexico: American Association of Petroleum Geologists Bulletin, v. 49, p. 2041-2075.

Baltz, E. H., and Myers, D. A., 1999, Stratigraphic framework of upper Paleozoic rocks, southeastern Sangre de Cristo Mountains, New Mexico, with a section on speculations and implications for regional interpretation of Ancestral Rocky Mountains paleotectonics: New Mexico Bureau of Mines and Mineral Resources, Memoir 48, 269 p.

Casey, J. M., 1980, Depositional systems and paleogeographic evolution of the Late Paleozoic Taos Trough, northern New Mexico; in Fouch, T. D. and Magathan, E. R., eds., Paleozoic paleogeography of west-central United States: SEPM Rocky Mountain Section, West-Central United States Paleogeography Symposium, p. 181-196.

Emery, D. and Myers, K. J., eds., 1996, Sequence stratigraphy: Blackwell Science Ltd, London, 297 p.

Heckel, P. H., 2003, Updated cyclothem constraints on radiometric dating of the Pennsylvanian succession in North America and its correlation with dates from Europe: Newsletter on Carboniferous Stratigraphy, v. 21, p. 12-20.

Kluth, C. F. and Coney, P. J., 1981, Plate tectonics of the Ancestral Rocky Mountains: Geology, v. 9, p. 10-15.

Kottlowski, F. E., 1968, Late Paleozoic sediments derived from Pedernal uplift: American Association of Petroleum Geologists Bulletin, v. 52, p. 537.

Kues, B. S., 1996, Guide to the Late Pennsylvanian paleontology of the upper Madera Formation, Jemez Springs area, north-central New Mexico: New Mexico Geological Society, 47th Field Conference, Guidebook, p. 169-188.

Lucas, S. G., Wilde, G. L., Robbins, S., and Estep, J. W., 2000, Lithostratigraphy and fusulinaceans of the type section of the Bursum Formation, Upper Carboniferous of south-central New Mexico: New Mexico Museum of Natural History and Science, Bulletin 16, p. 1-13.

Muir-Wood, H., and Cooper, G. A., 1960, Morphology, classification, and life habits of the Productoidea (Brachiopoda): Geological Society of America, Memoir 81, 447 p.

Myers, D. A., 1988, Stratigraphic distribution of some fusulinids from the Wild Cow and Bursum formations, Manzano Mountains, New Mexico: U. S. Geological Survey, Professional Paper 1446-B, p. 23-65

Newell, N. D., 1937, Late Paleozoic pelecypods, Pectinacea: Kansas State Geological Survey, v. 10, pt. 1, 123 p.

Pettijohn, F. J., Potter, P. E. and Siever, R., 1987, Sand and Sandstone (2nd ed). Springer-Verlag, New York, 553 p.

Rollins, H. B, Carothers, M., and Donohue, J., 1979, Transgression, regression and fossil community succession: Lethaia, v. 12, p. 89-104.

Sanderson, G. A., Verville, G. J., Groves, J. R., and Wahlman, G. P., 2001, Fusulinacean biostratigraphy of the Virgilian Stage (Upper Pennsylvanian) in Kansas: Journal of Paleontology, v. 75, p. 883-887.

Soegaard, K., 1990, Fan-delta and braid-delta systems in Pennsylvanian Sandia Formation, Taos trough, northern New Mexico: Depositional and tectonic implications: Geological Society of America Bulletin, v. 102, p. 1325-1343.

Stevens, C. H., 1971, Distribution and diversity of Pennsylvanian marine faunas relative to water depth and distance from shore: Lethaia, v. 4, p. 403-412.

Sutherland, P. K., 1963, Paleozoic rocks: New Mexico Bureau of Mines and Mineral Resources, Memoir 11, p. 22-46.

Sutherland, P. K., 1972, Pennsylvanian stratigraphy, southern Sangre de Cristo Mountains, New Mexico; in Mallory, W. W. et al., eds., Geologic atlas of the Rocky Mounatin region: Denver, Rocky Mountain Association of Geologists, p. 139-142

Sutherland, P. K. and Harlow, F. H., 1973, Pennsylvanian brachiopods and biostratigraphy in southern Sangre de Cristo Mountains, New Mexico: New Mexico Bureau of Mines and Mineral Resources, Memoir 27, 173 p.

Van Wagoner, J. C., Mitchum, R. M., Campion, K. M. and Rahmanian, V. D., 1999, Siliciclastic sequence stratigraphy in well logs, cores, and outcrops: Concepts for high-resolution correlation of time and facies: AAPG Methods in Exploration Series, no. 7, 55 p.

Wahlman, G. P., 1998, Fusulinid biostratigraphy of the new Pennsylvanian-Permian boundary in the Southwest and Midcontinent USA: Geological Society of America, Abstracts with Programs, v. 30, no. 3, p. 34.